

# A Caratheodory-Fejer Approach to Dynamic Appearance Modeling \*

Hwasup Lim

Octavia I. Camps

Mario Sznaier

*Dept. of Electrical Engineering  
The Pennsylvania State University  
University Park, PA 16802*

## Abstract

*This paper presents a technique to learn dynamic appearance models from a small number of training frames. Under this framework, dynamic appearance is modelled as an unknown operator that satisfies certain interpolation conditions and that can be efficiently identified using very little a priori information with off the shelf software. The advantages of the proposed method are illustrated with several examples where the learned dynamics accurately predict the appearance of the targets preventing tracking failures due to occlusion or clutter.*

## 1 Introduction

A requirement common to most dynamic vision applications is the ability to track objects in a sequence of frames. Arguably, one of the most important challenges to successfully track a target is to overcome changes of its appearance that might occur over time. These changes, including size, shape and color can be due to several factors such as target motion, self-occlusion, target articulations, and changes in illumination.

Several researchers have proposed methods to design flexible tracking algorithms. Robustness can be improved by integrating over time the correspondences between individual frames and exploiting the dynamical properties of the target with a Kalman, unscented Kalman or particle filter [1–4]. Key to the success of these approaches is to have accurate dynamic models of the target [4].

Many of these approaches focus on tracking the position of the target and only address changes in appearance indirectly by using probabilistic methods to compare the target to some nominal template using for example pixel statistics [5–8]. Other techniques focus on building adaptive appearance models. For example, Jepson *et. al.* [9] use an online EM algorithm to adapt the appearance of a target

template over time. Hager and Belhumeur [10], Black and Jepson [11] and Ho *et. al.* [12], among others, learn target appearance models using linear subspaces.

While successful in many scenarios, these approaches suffer from the fact that the obtained models tend to be too rigid and fail to capture the *dynamics* of the appearance changes. As a result, tracking remains susceptible to incorrect measurements due for example to partial or self occlusion. This lack of robustness is illustrated in Figure 1 showing the effects of appearance change. The figure shows a few frames from a sequence where a blue and red football is tossed in the air. The two rows show results for tracking the ball using a combination of Kalman Filter with motion dynamics identified using Caratheodory Fejer, a method that was shown to be very robust to occlusion [4]. In the first row, the measurements were obtained using mean shift [7] to compare the color distribution of the target against its initial distribution. Since initially, only the blue side of the ball is visible, this approach fails to track the ball when it becomes red. In the second row, the measurements were obtained by using a search window where the color distribution is updated using the previous frame. While this approach can cope with color change as long as the ball remains visible, it fails to recover after the ball is occluded. This is due to a combination of two facts: i) the visible color of the ball at the time when the ball comes out from below the table (red) is different to the visible colors just before the occlusion (blue) and ii) the binder on the table is similar in color to the blue on the ball.

In this paper we show that all of the above issues can be addressed by identifying the *dynamics* of the appearance changes from a small number of initial frames. This is accomplished by reducing the problem of learning the appearance models to that of establishing the existence of an  $\ell_2$  to  $\ell_2$  operator that satisfies certain interpolation conditions. This allows for exploiting convex analysis and integral quadratic constraints methods recently developed (mostly in the control community) to recast the problems into a Linear Matrix Inequality (LMI) optimization form that can be efficiently solved in *real time* using commer-

---

\*This work was supported in part by NSF grants IIS 00117387, ECS 0221562, and IIS ITR 0312558

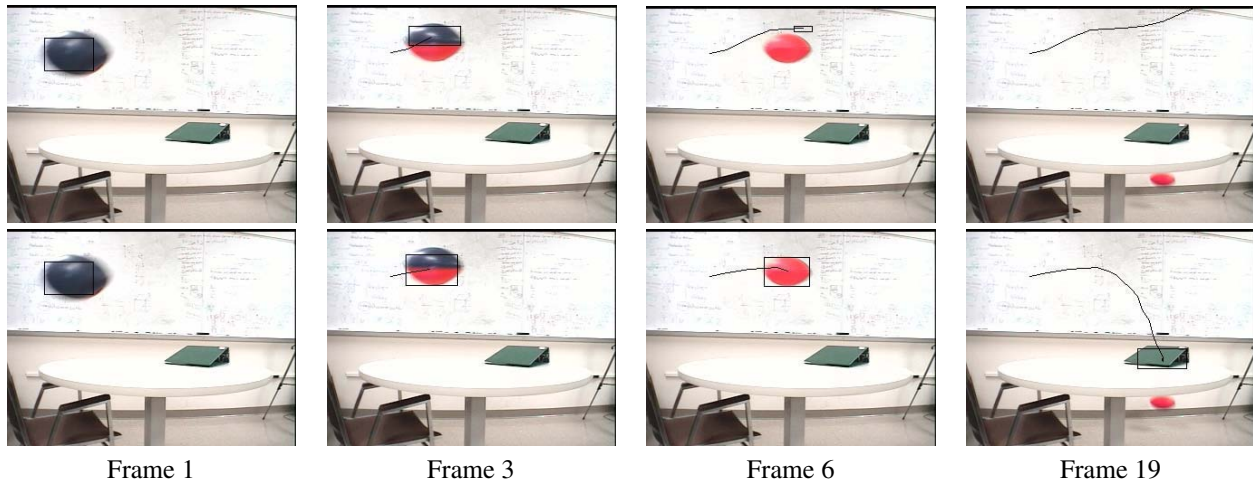


Figure 1. Color statistics from the first frame (top) and from the previous frame (bottom) fail to track a red and blue ball.

cially available tools.

The benefits of using this new framework are multiple: 1) It allows to approach the modeling and the tracking problems from an input – output point of view. Thus, it does not require prior knowledge of a state space realization of the system, or even its order. 2) It allows to naturally incorporate knowledge of the system dynamics whenever it is available. 3) It can learn the relevant dynamics from a few initial frames in the video sequence in real time. and 4) as we illustrate with several examples, the proposed method can be combined with existing particle and unscented Kalman filtering techniques leading to algorithms capable of robustly tracking targets with changing appearance, even in the presence of severe occlusion. When compared to existing techniques this combination allows for significantly improving robustness, while at the same time reducing the computational complexity of the resulting algorithm.

The paper is organized as follows. Section 2 provides a brief introduction to robust system identification. Section 3 states how the problem of learning appearance models can be posed as an interpolation one and shows that it can indeed be recast as an LMI problem by invoking Carathéodory-Fejér interpolation theory, and efficiently solved. Section 4 illustrates the proposed technique with several examples. Section 5 presents some conclusions and possible directions for future research.

## 2 Robust System Identification

The field of system identification concerns itself with mechanisms and algorithms that process finite, partial, and corrupted data to yield abstract mathematical descriptions of real world systems.

Traditional identification approaches [13] assume that

the data is corrupted by a stochastic process with known statistical properties and that the system to be identified has a prescribed model structure. Most of these identification procedures are based on least squares methods that estimate the parameters of the hypothesized models from the corrupted measurements. In these approaches the only source of uncertainty is the noise in the measurements while the prescribed model is assumed to be an accurate representation of the real system.

In many situations, for example when measurements are known within an accuracy range or when the available statistical information might be questionable, deterministic bounded noise descriptions are a practical and sound alternative to stochastic ones. Using this approach, the problem of system identification can be formulated as finding the sets of parameter values that are consistent with the known noise bounds. A survey of set membership formulations for system identification can be found in [14].

Other important factor affecting the quality of an identified model is the unrealistic presumption that a fixed model structure may fully represent the system to be identified: In practice, only partial information of the physical system is available, model parameters might change due to different operation conditions, and real systems are often too complex to be accurately modelled from first principles. These issues are addressed by *robust system identification* [15, 16], which departs from traditional approaches by using a **deterministic worst-case** approach with no prior assumption about the order of the system. Instead, robust identification procedures are based on *a priori* assumptions on the *class* of systems and noise and on the *a posteriori* experimental data. Using this information robust system identification algorithms find nominal models based on the experimental data and worst-case identification error bounds over the set

of models defined by the *a priori* information.

Due to the fact that the assumed *a priori* information is, in general, a quantification of the engineering common sense or simply a “leap of faith”, there is no guarantee that it will be coherent with the *a posteriori* experimental data. Thus, robust identification procedures must always first test the *consistency* of both types of information. Once consistency has been established, the computation of a nominal model and a valid model error bound can be attempted. In this paper we will concentrate on a specific class of algorithms, interpolatory [17], that allow for efficiently accomplishing all of these tasks. In addition, these algorithms are always guaranteed to converge as the information is completed. Finally, as shown in [15], they are optimal up to a factor of 2, in the sense that their worst-case error is never larger than twice the minimum achievable error over the set of all identification algorithms.

## 2.1 Notation

Below we summarize the notation used in the remainder of the paper:

$\mathbf{x}$	real-valued column vector.
$x_k$	$k^{\text{th}}$ element of a vector $\mathbf{x}$ .
$\ \mathbf{x}\ _p$	$p$ -norm of a vector: $\ \mathbf{x}\ _p \doteq (\sum_{k=1}^m  x_k ^p)^{\frac{1}{p}}$ , $p \in [1, \infty)$ , $\ \mathbf{x}\ _\infty \doteq \max_{k=1, \dots, m}  x_k $ .
$A^T$	conjugate transpose of matrix $A$ .
$\bar{\sigma}(A)$	maximum singular value of the matrix $A$ .
$A > 0$	$A = A^T$ is positive definite, i.e. $\mathbf{x}^T A \mathbf{x} > 0 \forall \mathbf{x} \in \mathbb{C}^n$ , $\mathbf{x} \neq \mathbf{0}$ .
$\mathcal{B}\mathcal{X}(\gamma)$	open $\gamma$ -ball in a normed space $\mathcal{X}$ : $\mathcal{B}\mathcal{X}(\gamma) = \{x \in \mathcal{X} : \ x\ _{\mathcal{X}} < \gamma\}$ .
$\mathcal{B}\mathcal{X}$	open unit ball in $\mathcal{X}$ .
$\ell_p^m$	extended Banach space of vector valued real sequences equipped with the norm: $\ x\ _p \doteq (\sum_{i=0}^{\infty} \ x_i\ _p^p)^{\frac{1}{p}}$ $p \in [1, \infty)$ and $\ x\ _\infty \doteq \sup_i \ x_i\ _\infty$ .
$\mathcal{L}_\infty$	Lebesgue space of complex-valued matrix functions essentially bounded on the unit circle, equipped with the norm: $\ G\ _\infty \doteq \text{ess sup}_{ z =1} \bar{\sigma}(G(z))$ .
$\mathcal{H}_\infty$	subspace of functions in $\mathcal{L}_\infty$ with bounded analytic continuation inside the unit disk, equipped with the norm: $\ G\ _\infty \doteq \text{ess sup}_{ z <1} \bar{\sigma}(G(z))$ .
$\mathcal{H}_{\infty, \rho}$	space of transfer matrices analytic in $ z  \leq \rho$ , equipped with the norm $\ G\ _{\infty, \rho} \doteq \sup_{ z <\rho} \bar{\sigma}(G(z))$ .
$X(z)$	$Z$ -transform of a right-sided real sequence $\{x\}$ : $X(z) = \sum_{i=0}^{\infty} x_i z^i$ .

In this paper, dynamic properties of targets – such as time evolution of its appearance, will be represented using linear operators responding to some input signal  $u$ , with outputs  $y$ . The outputs are sequences of time values of measured quantities, such as the target position, size, or gray value.

From an input–output viewpoint any linear operator of interest  $S$  will be represented by its convolution kernel  $\{s_{i,j}\}$  or by an infinite lower triangular matrix  $T_S$  mapping (scalar) sequences in  $\ell_2$ :

$$\begin{bmatrix} y_0 \\ y_1 \\ y_2 \\ \vdots \end{bmatrix} = \begin{bmatrix} s_{0,0} & 0 & 0 & \dots \\ s_{1,0} & s_{1,1} & 0 & \dots \\ s_{2,0} & s_{2,1} & s_{2,2} & \dots \\ \vdots & \vdots & \vdots & \ddots \end{bmatrix} \begin{bmatrix} u_0 \\ u_1 \\ u_2 \\ \vdots \end{bmatrix}. \quad (1)$$

When dealing with input–output sequences on the horizon  $[0, n-1]$ , we will use the finite upper left submatrix of  $n \times n$ ,  $T_S^n$ , obtained from the infinite matrix above.

In the sequel, we will also represent finite dimensional Linear Time Invariant (LTI) operators by using either a minimal state–space realization:

$$\begin{aligned} \mathbf{x}_{k+1} &= A\mathbf{x}_k + B u_k \\ y_k &= C\mathbf{x}_k + D u_k \end{aligned} \quad (2)$$

or a (rational) complex-valued transfer function:  $S(z) \doteq \sum_{k=0}^{\infty} s_k z^k$ .

## 2.2 CF Identification Algorithm

In this section we briefly review the properties of the Caratheodory-Fejer interpolatory identification algorithm used in the paper.

In the sequel we consider operator families of the form  $\mathcal{S}$ :

$$\mathcal{S} \doteq \{S(z) = F_{n_p}(z) + F_p(z)\} \quad (3)$$

where operators  $S(z)$  are described in terms of a *nonparametric* component  $F_{n_p}(z) \in \mathcal{B}\mathcal{H}_\infty(K)$  and a *parametric* component  $F_p(z)$ . We will further assume that the parametric component  $F_p(z)$  belongs to the following class  $\mathcal{P}$  of affine operators:

$$\mathcal{P} \doteq \{P(z) = \sum_{i=1}^{N_p} p_i F^i(z) = \mathbf{p}^T \Phi(z), \mathbf{p} \in \mathcal{R}^{N_p}\}, \quad (4)$$

where the  $N_p$  components  $F^i(z)$  of vector  $\Phi(z)$  are known, linearly independent, rational transfer functions.

The next lemma gives a necessary and sufficient condition for two finite vector sequences to be related by an operator in the family  $\mathcal{S}$ .

**Lemma 1.** Given a scalar  $K$ , and two vector sequences  $(\mathbf{u}, \mathbf{y})$ , there exists an operator  $S \in \mathcal{S}$  such that  $\mathbf{y} = S\mathbf{u}$  if and only if there exists a pair of vectors  $(\nu, \mathbf{p})$  satisfying:

$$M(\nu) \doteq \begin{bmatrix} 1 & (\mathbb{T}_\nu^N)^T \\ \mathbb{T}_\nu^N & \frac{1}{K^2} \end{bmatrix} \geq 0 \quad (5)$$

$$\mathbf{y} = \mathbb{T}_u \mathbf{P} \mathbf{p} + \mathbb{T}_u \nu$$

where  $(\mathbf{P})_k \doteq [F_k^1 \ F_k^2 \ \dots \ F_k^{N_p}]$ , with  $F_k^i$  denoting the  $k$ -th Markov parameter of the  $i$ -th transfer function  $F^i(z)$ ,  $\nu_k$  the  $k$ -th Markov parameter of the nonparametric component  $F_{np}(z)$ , respectively, and the scalar  $K$  is an upper bound of the  $\ell_2$  induced norm of  $F_{np}(z)$ .

Moreover, in this case all such operators  $S$  can be parameterized in terms of a free parameter  $Q(z) \in \mathcal{BH}_\infty$ . In particular, the choice  $Q(z) = 0$  leads to the ‘‘central’’ model  $S_{central}(z) = F_{np_o}(z) + \mathbf{p}^T \Phi(z)$  where an explicit state–space realization of  $F_{np_o}(z)$  is given by:  $F_{np_o}(z) = C_F(zI - A_F)^{-1} B_F + D_F$  with

$$A_F = \left\{ A - [C_-^T C_- + (A^T - I)]^{-1} C_-^T C_- (A - I) \right\}^{-1}$$

$$B_F = [C_-^T C_- (A^T - A - I) - (A^T - I)A]^{-1} C_-^T$$

$$C_F = KC_+ - KC_+ \left\{ A - [C_-^T C_- + (A^T - I)]^{-1} C_-^T C_- (A - I) \right\}^{-1}$$

$$D_F = KC_+ \left\{ [C_-^T C_- + (A^T - I)]A - C_-^T C_- (A - I) \right\}^{-1} C_-^T$$

$$A = \begin{bmatrix} 0 & I_{N \times N} \\ 0 & 0 \end{bmatrix}, \quad C_- = \overbrace{[1 \ 0 \ \dots \ 0]}^{N+1}, \quad C_+ = \frac{\nu^T}{K}. \quad (6)$$

*Proof.* See Theorem 18.5.2 in [18] and [19].  $\square$

Finally, the following corollary addresses the issue that real plants are subject to some unknown but bounded noise.

**Corollary 1.** [19] Consider the problem of identifying an operator  $S \in \mathcal{S}$  from measurements of its output  $y$  to a known input  $u \in \ell_2[0, N]$ , corrupted by additive bounded noise  $\eta$  in a given set  $\mathcal{N}$ :

$$y_k = (S * u)_k + \eta_k, \quad k = 0, 1, \dots, N. \quad (7)$$

Then there exist  $S \in \mathcal{S}$  that satisfies (7) if and only there exists a pair of vectors  $(\nu, \mathbf{p})$  such that  $M(\nu) > 0$  and  $\mathbf{y} - \mathbb{T}_u \mathbf{P} \mathbf{p} - \mathbb{T}_u \nu \in \mathcal{N}$ . In that case, one such operator is given by  $S_{central} = \mathbf{p}^T \Phi + F_{np_o}$ , where  $F_{np_o}$  has the state–space realization (6).

### 3 Learning Appearance Models

In this section we show that the problem of learning the appearance model of a target from a sequence of frames is

equivalent to finding an  $\ell_2$  to  $\ell_2$  operator that satisfies certain interpolation conditions. This approach allows for appealing to integral quadratic constraints (IQCs) [20], convex analysis and interpolation concepts to recast these problems into a tractable LMI optimization form.

As mentioned in the introduction, changes in the appearance of a target can cause tracking failure, specially in the presence of clutter and occlusions. As we show next, these difficulties can be solved by modelling the appearance of the target as the output of an ARMA model and using the results in section 2 to identify the relevant dynamics.

Specifically, assume that the present value of a given appearance descriptor of the target, such as size, number of pixels of a given hue, or hue of a given pixel,  $f_k$  is related to its past  $N$  values by<sup>1</sup>:

$$\begin{aligned} f_k &= \mathcal{A}f + \mathcal{B}u \\ y_k &= f_k + \eta_k \end{aligned} \quad (8)$$

where  $\mathbf{f} = (f_{k-1} \ \dots \ f_{k-N})^T$  contains the past observations of the descriptor,  $\mathbf{u} = (u_k \ u_{k-1} \ \dots \ u_{k-m})^T$  represents a stochastic input,  $y_k$  denotes the available measurement of the descriptor, corrupted by noise  $\eta_k$ , and where  $\mathcal{A}$  and  $\mathcal{B}$  are suitable LTI operators. Alternatively, (by taking  $z$ -transforms in the equation above), one can use the description:

$$y(z) = F(z)u(z) + \eta(z) \quad (9)$$

where the operator  $F$  is not necessarily  $\ell_2$  stable. In the sequel, we will assume that the following *a priori* information is available:

1. A set membership description of the process noise and the measurement:  $\eta_k \in \mathcal{N}$  and  $u_k \in \mathcal{U}$ . These sets can be used to impose correlation constraints.
2. The operator  $F$  admits a finite expansion of the form  $F = F_p + F_{np}$ , where  $F_p = \sum_{j=1}^n p_j F^j$  with  $F^j$  known, given, not necessarily  $\ell_2$  stable operators that contain all the information available about possible modes of the descriptor of the target appearance<sup>2</sup>.
3. The residual operator  $F_{np} \in \mathcal{BH}_{\infty, \rho}(K)$  for some known  $\rho \leq 1$ . That is, a worst case estimate is available of how fast the approximation error of the finite expansion  $F_p = \sum_{j=1}^n p_j F^j$  diverges.

<sup>1</sup>For simplicity, we consider a single descriptor, but the equations generalize trivially to the multiple–descriptor case.

<sup>2</sup>If this information is not available the problem reduces to purely non–parametric identification by setting  $F^j \equiv 0$ .

In this context, the next value of the appearance descriptor  $f_k$  can be predicted by first identifying the relevant dynamics  $F$  and then using it to propagate its past  $N$  values. In turn, identifying the dynamics entails finding an operator

$$F(z) \in \mathcal{S} \doteq \{F(z): F = F_p + F_{np}\}$$

such that  $y - \eta = F'u$ , precisely the class of interpolation problem addressed in Corollary 1 in section 2. By noticing that

$$F_{np}(z) \in \mathcal{BH}_{\infty, \rho} \iff F_{np}\left(\frac{z}{\rho}\right) \in \mathcal{BH}_{\infty},$$

it follows that such an operator exists if and only if the following set of equations is feasible:

$$\begin{aligned} M_R(\nu) &= \begin{bmatrix} R_\rho^2 & T_\nu^T \\ T_\nu & K^2 R_\rho^{-2} \end{bmatrix} \geq 0 \\ \mathbf{y} - T_u P \mathbf{p} - T_u \nu &\in \mathcal{N} \end{aligned} \quad (10)$$

where  $R_\rho \doteq \text{diag}[1 \ \rho \ \dots \ \rho^N]$ .

This is a linear matrix inequality (LMI) problem that can be efficiently solved using commercial software such as the LMI Matlab toolkit.

## 4 Illustrative Examples

In this section we present several examples to illustrate how the proposed approach can be used to improve the robustness of trackers in the presence of appearance changes. In all the given examples, the tracking algorithm combined Kalman filters with appearance and motion dynamics learned using the proposed CF-based identification algorithm.

In the first two examples, the proposed technique was used to track multicolored balls. In both cases, the *bin counts of the hue histogram of the target* were used as appearance descriptors. These histograms were computed in small regions determined by a mean shift algorithm comparing the hue values of the region against the current estimates of the hue histograms.

Proceeding as described in the previous section, we used a combination of *a priori* information:

1. 10% noise level for the appearance parameters and 3% for the location coordinates of the target.
2.  $\mathcal{E} = \delta(0)$ , i.e. the histogram bin counts and the location coordinates of the target were modelled as the impulse response of unknown operators  $F$
3. The parametric parts of the operators must satisfy:  $F_p \in \text{span}\left[\frac{1}{z+1}, \frac{z}{(z-1)^2}, \frac{z^2 - \cos \omega z}{z^2 - 2 \cos \omega z + 1}\right]$  where  $\omega \in \{0.1, 0.12, 0.55\}$

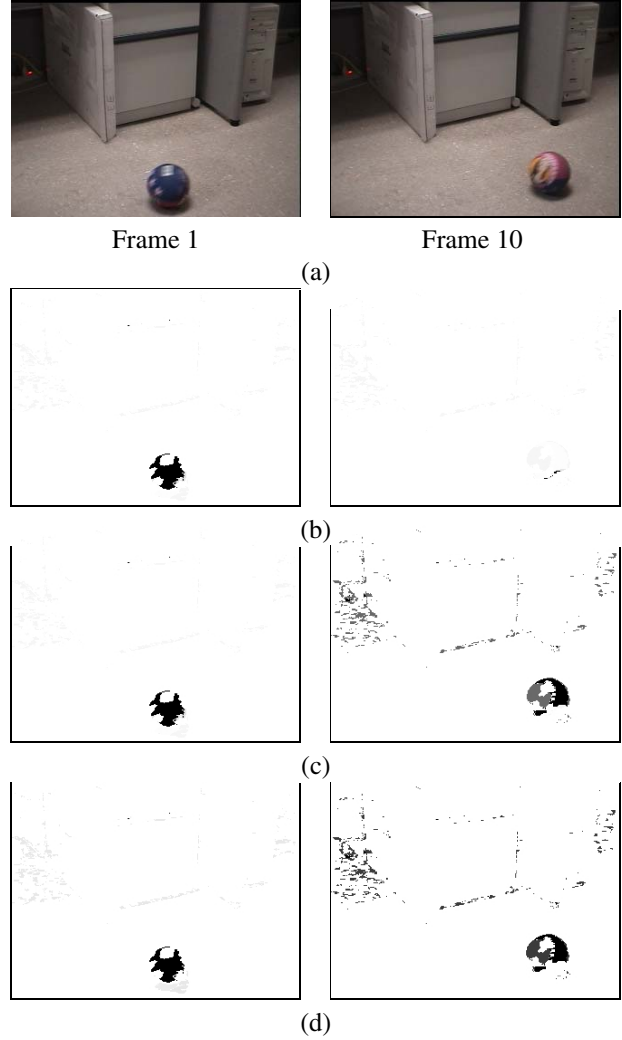


Figure 2. CF-based appearance learning: (a) First frame (the ball is mostly blue), and tenth frame (a mix of orange, blue and red). (b) to (d) probability of a pixel belonging to the ball, according to the histogram from the (b) first frame; (c) previous frame and (d) predicted by the CF-based dynamic appearance model.

4. The remainder, nonparametric components, which explains the unmodelled dynamics satisfies  $F_{np} \in \mathcal{BH}_{\infty, \rho}(K)$ , with  $\rho = 0.99$

and the *a posteriori* measurements from  $N = 21$  frames, where the target was not occluded, to estimate their dynamics. These dynamics were then used in conjunction with Kalman filters, leading to the results shown in Figures 3 to 4.

In the first example, a colorful ball was rolled in front of the camera. Figure 2 (a) shows two frames of this sequence. In the first frame, the visible part of the ball is mostly blue while in the tenth frame its visible part is a mix of orange,

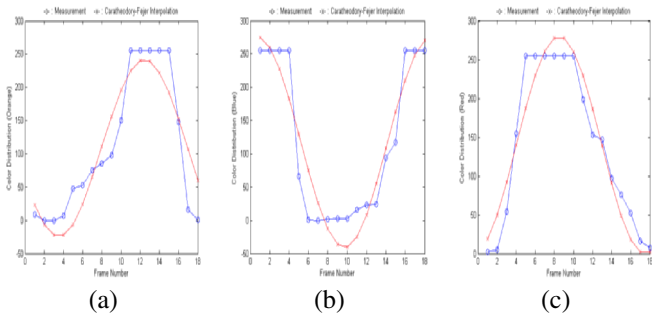


Figure 3. Measurements and CF estimated values of the (a) orange, (b) blue and (c) red bin counts of the hue histogram of the ball shown in Figure 2(a) as it rolls in front of the camera.

blue, and red.

Figures 3 (a), (b) and (c) show plots of the measured and predicted values for the orange, blue and red bins, respectively, of the hue histogram of this colorful ball as it rolls in front of the camera.

Figures 2 (b) to (d) show the probabilities (darker pixels correspond to higher probabilities) of the image pixels belonging to the ball according to the histogram from the first frame, the histogram from the previous frame, and the histogram predicted by the CF-based dynamic appearance model, in (a), (b) and (c) respectively. It is seen that using the initial histogram will result in missing the ball in the tenth frame. Updating the histogram using the previous frame performs better, and using the histogram predicted from the CF-based identified appearance model performs the best with more pixels with high probability within the ball.

The next two examples illustrate the robustness of the CF-based dynamic model in the presence of occlusion. Figure 4 shows the tracking results when the CF-based dynamic appearance model is used in the sequence shown before in Figure 1. As it is seen here, the new approach is able to track the ball beyond the occlusion. This is possible due to the accurate appearance predicted by the learned model as illustrated in Figure 5. Notice that there are no measurements while the ball was occluded behind the table, but once they become available again, there is a close match between measurements and predicted values. In Figure 6 the proposed method was used to learn the dynamics of the *size* of the target in a sequence where a car approaches the camera. In this case, the appearance descriptors used were the *vertical and horizontal sizes* of a box around the target which was found by comparing the hue histogram of the target against the initial hue histogram with a mean shift algorithm (i.e. it was assumed that the colors of the target are approximately constant). The figure shows how the tracking algorithm recovers the target after the occlusion and that

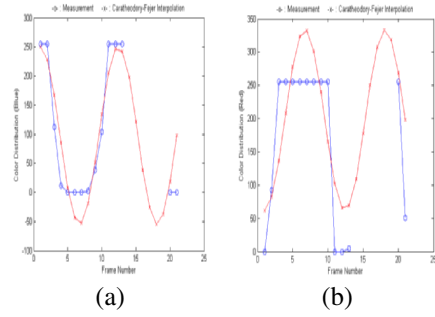


Figure 5. Measurements and CF estimated values the (a) blue, and (b) red bin counts of the hue histogram of the ball shown in Figure 4 as it flies in front of the camera.

the box around the target is of the right size.

Finally, it should be noted that a salient feature of these results is the fact that the combination Caratheodory–Fejer/Kalman Filter achieved virtually the same performance as CF/UPF and substantially outperforms the UPF alone. Thus the proposed approach can both improve robustness and alleviate the computational complexity of the problem.

## 5 Conclusions

In the past few years dynamic vision techniques have proved to be a viable option for a large number of applications, ranging from surveillance and manufacturing to assisting individuals with disabilities. Arguably, at this point one of the critical factors limiting widespread use of these techniques is the potential fragility of the systems when the target changes appearance. In this paper we show that this fragility can be addressed by using interpolation and LMI tools recently developed in the control community to recast these problems into a tractable optimization form. The advantages of this approach, and in particular its potential to result in robust algorithms when combined with existing tracking techniques was illustrated with several experimental results. Research is currently underway seeking to combine the proposed technique with mixed  $\mathcal{H}_2/\mathcal{H}_\infty$  filters in an attempt to better capture the properties of the problem.

## References

- [1] M. Isard and A. Blake, “CONDENSATION – conditional density propagation for visual tracking,” *IJCV*, vol. 29, no. 1, pp. 5–28, 1998.
- [2] B. North, A. Blake, M. Isard, and J. Rittscher, “Learning and classification of complex dynamics,” *IEEE Trans. PAMI*, vol. 22, no. 9, pp. 1016–1034, September 2000.

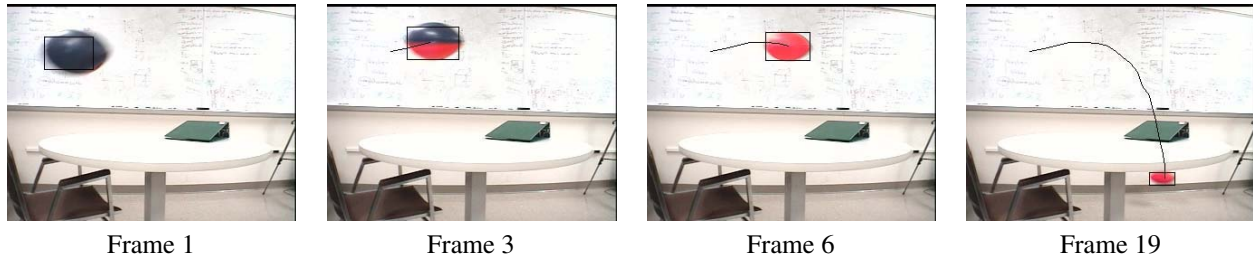


Figure 4. CF-based dynamical appearance model. Tracking using dynamical appearance and motion models of a red and blue ball is successful, even in the presence of occlusion. See text for details.



Figure 6. Approaching car example. An increasing size car is successfully tracked in the presence of occlusion by using CF-based identification to learn the size and the motion dynamics of the target.

- [3] S. Julier, J. Uhlmann, and H. F. Durrant-Whyte, "A new approach for filtering nonlinear systems," in *Proc. of the 1995 ACC*, 1995, pp. 1628–1632.
- [4] O. I. Camps, H. Lim, C. Mazzaro, and M. Sznaiier, "A Caratheodory–Fejer approach to robust multiframe tracking," in *ICCV*, Nice, France, October 2003, pp. 1048–1055.
- [5] P. Perez, C. Hue, J. Vermaak, and M. Gangnet, "Color-based probabilistic tracking," in *7th ECCV*, 2002, pp. 661–675.
- [6] D. Comaniciu, V. Ramesh, and P. Meer, "Real-time tracking of non-rigid objects using mean shift," in *IEEE CVPR*, June 2000, pp. 142–149.
- [7] G. R. Bradski and V. Pisarevsky, "Intel's computer vision library: applications in calibration, stereo, segmentation, tracking, gesture, face and object recognition," in *IEEE CVPR*, vol. II, 2000, pp. 796–797.
- [8] Z. Zivkovic and B. Krose, "An EM-like algorithm for color-histogram-based object tracking," in *CVPR*, vol. 1, June 2004, pp. 798–803.
- [9] A. D. Jepson, D. J. Fleet, and T. F. El-Maraghi, "Robust online appearance models for visual tracking," *IEEE Trans. PAMI*, vol. 25, no. 10, pp. 1296–1311, 2003.
- [10] G. Hager and P. Belhumeur, "Efficient region tracking with parametric models of geometry and illumination," *IEEE Trans. PAMI*, vol. 20, no. 10, pp. 1025–1039, 1997.
- [11] M. J. Black and A. D. Jepson, "Eigentracking: Robust matching and tracking of articulated objects using a view-based representation," *IJCV*, vol. 26, no. 1, pp. 63–84, 1998.
- [12] J. Ho, K. C. Lee, M. H. Yang, and D. Kriegman, "Visual tracking using learned linear subspaces," in *IEEE CVPR*, vol. 1, June 2004, pp. 782 – 789.
- [13] L. Ljung, "Development of system identification," in *IFAC Congress*, vol. G, 1996, pp. 141–146.
- [14] M. Milanese and A. Vicino, "Optimal estimation theory for dynamic systems with set membership uncertainty: an overview," *Automatica*, vol. 27, pp. 997–1009, 1991.
- [15] R. Sánchez Peña and M. Sznaiier, *Robust Systems Theory and Applications*. Wiley & Sons, Inc., 1998.
- [16] J. Chen and G. Gu, *Control Oriented System Identification, An  $\mathcal{H}_\infty$  Approach*. New York: John Wiley, 2000.
- [17] J. Chen, C. Nett, and M. Fan, "Worst-case system identification in  $\mathcal{H}_\infty$ : Validation of *a Priori* information, essentially optimal algorithms and error bounds," *IEEE Trans. on Autom. Contr.*, vol. 40, no. 7, 1995.
- [18] J. Ball, I. Gohberg, and L. Rodman, *Interpolation of Rational Matrix Functions, Operator Theory: Advances and Applications*. Birkhäuser, Basel, 1990, vol. 45.
- [19] P. A. Parrilo, R. S. S. Pena, and M. Sznaiier, "A parametric extension of mixed time/frequency domain based robust identification," *IEEE Trans. Autom. Contr.*, vol. 44, no. 2, pp. 364–369, 1999.
- [20] A. Megretski and S. Treil, "Power distribution inequalities in optimization and robustness of uncertain systems," *J. of Mathematical Systems, Estimation and Control*, 1993.